Available online at website: https://journal.bcrec.id/index.php/bcrec

Bulletin of Chemical Reaction Engineering & Catalysis, 21 (3) 2026, 638-645

Original Research Article

Apparent Reaction Kinetics of Crude Palm Oil Dechlorination Using Sodium Silicate Solution

Zulfa Kurnia Umani Binti Hari, Nur Shafikah Binti Rasad, Mohd Sabri Bin Mahmud*

Faculty of Chemical and Process Engineering Technology, Universiti Malaysia Pahang Al-Sultan Abdullah, Lebuh Persiaran Tun Khalil Yaakob, Gambang, 26300 Kuantan, Pahang, Malaysia.

Received: 18th March 2026; Revised: 25th April 2026; Accepted: 26th April 2026
Available online: 16th June 2026; Published regularly: October 2026

Abstract

This paper reports a study of the apparent reaction kinetics of crude palm oil (CPO) dechlorination using a sodium silicate (SS) solution, providing a water-efficient alternative to conventional washing to mitigate the 3-MCPD precursor. Three CPO-to-SS volume ratios (0.25, 2.33, and 3.00) were tested across temperatures of 60 °C, 70 °C, and 80 °C. The results showed the 2.33 ratio as most effective, achieving 1000 times of extraction, as indicated by the McCabe-Thiele equilibrium plot. Kinetic analysis revealed a transition from pseudo-first-order regimes at lower temperatures to exceptionally high apparent reaction orders (up to 24.90) at 80 °C. These high orders indicate a mass-transfer limited process where declining SS concentration might have destabilized the emulsion, making the reaction rate sensitive to interfacial surface area. The FTIR spectra confirmed that SS acted as both a buffering agent and a dispersant, reducing moisture retention without clear free fatty acid neutralization. The elevated temperatures significantly enhanced dechlorination rates, with the 0.25 ratio facilitating chloride breakdown with the highest rate constant. The results revealed that the kinetic rate is: $r = kC_{OH}^{\propto}$, with the rate constant, k (range 3.6×10^{-3} until 1×10^{-111}) and the apparent order,$\propto$ (range up to 24.9) at 80 °C. These findings conclude that SS can effectively reduce chlorine content in CPO, and that process is strongly governed by the phase volume ratio and operating temperature.

Keywords: crude palm oil dechlorination; dechlorination kinetics; 3-MCPD precursors; biphasic reaction; sodium silicate; chemical scavenger

How to Cite: Hari, Z. K. U., Rasad, N. S., Mahmud, M. S. (2026). Apparent Reaction Kinetics of Crude Palm Oil Dechlorination Using Sodium Silicate Solution. *Bulletin of Chemical Reaction Engineering & Catalysis*, 21 (3), 638-645. (DOI: 10.9767/bcrec.20687)

Permalink/DOI: https://doi.org/10.9767/bcrec.20687

1. Introduction

Palm oil is an important global edible oil. Its refining process can form harmful contaminants such as 3-monochloropropane-1,2-diol (3-MCPD) and its esters if chloride ion is present. The International Agency for Research on Cancer (IARC) classifies them as possibly carcinogenic to humans due to its association with renal tubular hyperplasia and benign tumors in animal studies [1]. This raises significant food safety concerns for palm oil industries.

Chlorine, particularly chloride ion, is key precursor to 3-MCPD, which exists in crude palm oil (CPO) as inorganic and organic chlorides. During high-temperature refining in the presence of strong acid, these compounds can transform into chlorinated esters, which subsequently degrade to form 3-MCPD [2]. Beyond safety risks, organic chlorides can accelerate rancidity, reducing shelf life and nutritional quality [3]. Therefore, controlling chlorine content is essential for ensuring both product safety and quality.

Current dechlorination practices, such as water washing, are widely applied in mills located near plantations where water is abundantly available [4]. However, this approach seems impractical for refineries located in industrial zones or port areas where free chlorine water may

* Corresponding Authors.
Email: mohdsabri@umpsa.edu.my (Mahmud, M. S.)

be scarce. Alternative methods, such as steam distillation and adsorption using silica, activated carbon or bleaching earth have been explored, but these techniques face considerable challenges, including hydrolysis of chlorides into corrosive hydrogen chloride and strict requirements for temperature and pressure regulation [5,6]. These limitations highlight the need for a more efficient, scalable and water-conversing solution.

From the review of literature, the information of chlorine distribution between CPO and it treating liquid phase is lacking. Despite several reports from dechlorination studies, none of them reported their dechlorinating agent between two contacting liquids and their reports only present simple raw data without any kinetic parameter that can be used to design the chlorinating unit of operation. Alkaline extraction provides a promising route to remove organic chlorides without relying on large volumes of water. However, the alkaline concentration must be sufficiently controlled to prevent unwanted saponification and hydrolysis reactions. In this study, sodium silicate (SS) was selected because it provides a buffering mechanism for sodium hydroxide released upon its dissociation according to Equations (1) and (2).

$$\underset{\text{Sodium Silicate}}{Na_2SiO_3} + 2H_2O \rightleftharpoons 2NaOH + \underset{\text{Silicic Acid}}{H_2SiO_3} \quad (1)$$

$$NaOH \rightarrow Na^+ + OH^- \quad (2)$$

Besides organic chloride, NaOH from SS can also react with inorganic chloride to form water-soluble, chloride salts, which then be separated from the oil phase. The efficiency of this reactive extraction depends on factors such as pH and distribution coefficients between oil and aqueous phases. To systematically evaluate these parameters, the McCabe–Thiele approach for liquid-liquid system is employed, providing insight into equilibrium relationships and the number of theoretical stages required for effective dechlorination [7,8]. The use of SS as a buffering agent for alkali may enhance pH stability, thereby promoting a new method for converting chlorides into less hazardous, water-soluble forms [9]. Therefore, comprehensive analysis of different mixture compositions and sodium-silica ratios is required to define the intricate chemical pathways involved in applying aqueous sodium silicate to CPO. This study aimed to delineate the apparent reaction kinetics of the reaction between hydroxide and chloride compound in CPO.

2. Materials and Method

2.1. Materials

CPO samples were collected from a final storage tank of the Felda-owned mill at Lepar Hilir, Kuantan, Pahang, Malaysia. The collected CPO was vigorously stirred to ensure homogeneity before being aliquoted into several containers and stored in a chiller for preservation. For each laboratory session, the required amount of CPO was thawed and stirred again to restore uniformity at room temperature, which was 29 °C. Sodium metasilicate (SS) with technical grade was supplied by Sigma-Aldrich. Deionized water was used to prepare 0.01 g/mL of SS solution, corresponding to concentration commonly applied in industrial practice [10].

2.2. Extraction of Chloride from CPO

Three volume ratios of CPO to SS solutions were prepared in 300 mL beakers, i.e. 3.0, 2.33, and 0.25, the ratios that could secure biphasic conditions in our previous work [11]. Prior to mixing, the pH of each liquid was measured. The oil and aqueous solutions were then combined and mixed using a tabletop overhead stirrer (DLAB, OS4-Pro) (200 rpm) and a magnetic stirrer (400 rpm) at room temperature to ensure vigorous mixing and rate limiting conditions. The pH of the mixture was measured using the pH meter (Mettler Toledo, FiveEasy model). After mixing, separation processes were carried out using a centrifuge at 5000 rpm for 15 minutes to separate liquid phases within 5 appropriate intervals. Thus, all centrifuged samples were left for an additional 15 minutes to ensure full phase separation and to minimize any remaining reactions. Each sample was collected carefully from both oil and aqueous phase by utilizing pipettes. Initial purging of air from submerged pipette tips was applied when the bottom liquid phase was taken. Each sample, either oil or aqueous phase, was analyzed using ThermoFisher FTIR and OMNIC software to quantify the free fatty acid level in both phases formed using the method proposed by Hari et al. [12]. Functional groups were also compared before and after the mixing. Chloride concentration in aqueous phase was determined by using a UV-Vis Spectrophotometer Merck Spectroquant Prove 300 and the total chlorine content in the oil phase was determined by using Combustion Ion Chromatography (CIC) Mitsubishi AQF-100, according to the ASTM D4929-19 standard. Total chlorine content covers inorganic chloride, organic chloride and radical chlorine but chloride content measured by the spectrophotometer only covers water-soluble chloride compounds such as inorganic chloride and radical chlorine. Initial known concentration of chloride ion in an aqueous sample was used to compare results of chloride content between the spectrophotometer and CIC.

2.3. Determination of Dechlorination Rate

Using the same mixture preparation and reaction setup as mentioned in Section 2.2, the

dechlorination rate test was conducted at three different temperatures: i.e. 60 °C, 70 °C, and 80 °C for each volume ratio, which are lower than operating temperatures at most units in mills [13]. The oil and alkaline buffer solution were heated separately by using the heating bath until the desired temperatures were achieved and both initial pH values were recorded. Then, the reaction started by mixing both liquids using tabletop and magnetic stirrer. The pH was recorded within the time intervals of 30, 60, 90, and 120 seconds as a measurement for hydroxide ion concentration. Hydroxide ions from NaOH are involved in a nucleophilic substitution with organic chlorides to form sodium chloride salt and alcohols. Although hydroxide ion was present in access compared to chloride components (ionic or organic compound), its concentration measurement was preferred thru pH analyses to represent the dechlorination. This approach was chosen partly due to the limited availability and higher cost of trace chloride content analysis [14]. Other analysis methods that need separate analyte solution preparations might involve human errors and the delay would produce wrong results mainly due to uncertainty related to the reversible reaction of SS dissociation. The measurement of chloride contents was not possible due to its traces level of concentration. The nucleophilic substitution reaction equation between sodium hydroxide and organic chloride is expressed in Equation (3). The samples were analyzed using the same methods in Section 2.2.

$$OH^- + RCl \rightarrow ROH + Cl^- \quad (3)$$

The rate of the dechlorination reaction was determined by differentiating the regression equations obtained from fitting the time-dependent OH^- concentration data using an exponential decay model [15].

3. Results and Discussion

3.1. Extraction of Chloride from CPO

Water-soluble chloride species and radical chlorine present in the aqueous solution were compared with total chlorine content in the oil to evaluate liquid-liquid extraction behavior based on the MacCabe-Theile method. In this system, CPO served as the original phase containing chlorine/chloride, while the aqueous phase acted as extractant. The distribution of chloride between the two phases was assessed relative to the operating line associated with each volume ratio to determine the extractability of the solute. Figure 1 shows the MacCabe Thiele plot for the CPO-water system and CPO-SS solution system using 0.01 g/L SS solution. y denotes composition of chlorine in CPO and x denotes the composition of chlorine (where soluble chlorines are chloride ions and radical chlorines) in SS. For the CPO-water system in Figure 1(a), the ratios of 7:3 and 3:1 produced chloride distribution points (equilibrium point or EP) below the respective operating lines (OL), whereas the 1:4 ratio yielded a point above the line, indicating that only the 1:4 ratio achieved extraction conditions when deionized water was used. In contrast, for the CPO-SS system shown by Figure 1(b), all chloride distribution points were positioned significantly above the operating line, demonstrating that by the presence of SS, greatly enhanced the extraction efficiency, which was more than 1000 times if both distributions of chloride are compared. The significant enhancement in extraction efficiency observed in the CPO-SS system is largely facilitated by the inherent

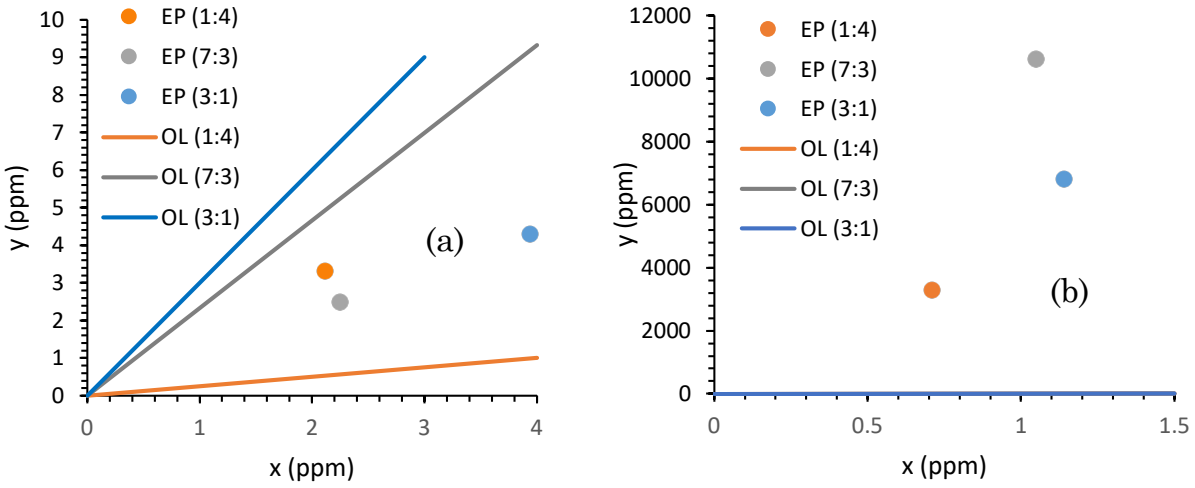

Figure 1. McCabe Thiele graphs of liquid-liquid extraction for (a) CPO-water system and (b) CPO-SS solution system.

buffering capacity of the sodium silicate solution. By maintaining a stable alkaline environment during the extraction, SS ensures that the pH remains within a range conducive to chloride solubility throughout the phase contact. This stability prevents the ionic fluctuations that would otherwise occur in a non-buffered system.

3.2. Infrared Radiation Analysis

The FTIR spectra contains a series of characteristic bands where wavenumbers and intensities reveal the functional groups present in oil and water samples. This is a mid-infrared region, typically has four main sections where the type of group frequency can often be inferred from the region in which it appears. These include the X–A stretching in the wavenumber from 4,000 to 2,500 cm^{-1}, the triple-bond region in 2,500 – 2,000 cm^{-1}, the double-bond region in 2,000 – 1,500 cm^{-1}, and the fingerprint region in 1,500 – 600 cm^{-1} [16].

Figure 2 presents overlayed attenuated total reflectance (ATR) spectra for CPO mixed with deionized water and SS solution at three different ratios, which were scanned from 600 to 4000 cm^{-1}. The characteristic transmittance features of oils were evident. Notably, the C-H stretching bands associated with cis C=CH, CH_2, CH_3 and CH_2/CH_3 groups appeared between 2,800 and 3,050 cm^{-1}. The strong C=O stretching vibration of the triacylglycerol ester linkage is evidenced in the 1,650 to 1,800 cm^{-1} region, while numerous structural vibrations constituting the typical fingerprint pattern occurred within 1000 – 1,500 cm^{-1} [17]. Distinct peaks attributed to nitrogen-associated stretching bands, which were normally absent in refine palm oil [18], appeared at various intensities from 2220 to 2280 cm^{-1} in both mixtures. The highest peak intensity was observed at the ratio of 3:1 for the CPO-water system and 1:4 for the CPO-SS system. The broad band observed between 3100 and 3600 cm^{-1} corresponds to O-H stretching from hydrogen bonding. While this region suggests significant aqueous interaction, the variations in environment and molecular ratio significantly influence these specific vibrational modes. Billa *et al.* [19] suggested hydrogen bonding can alter the intensity of nitrogen-containing functional groups, which explains the intensity increase observed in the 3:1 ratio. Furthermore, chemical modifications within the matrix may enhance specific vibrations, similar to phenomena observed in polyacrylonitrile fibers where modification alters C≡N and C=N peak intensities [20].

The infrared spectrum reveals that the presence of sodium silicate (SS) significantly altered the physicochemical interactions between crude palm oil (CPO) and the aqueous phase with and without SS as shown in Figure 2 and Figure 3, respectively. A reduced intensity of the O–H stretching band (3100–3600 cm^{-1}) in the CPO–SS system compared with the CPO–water system indicates lower moisture retention in the oil phase. This behavior can be attributed to a salting-out effect, whereby the increased ionic strength resulting from SS dissociation enhances water polarity and decreases the solubility of residual water in the oil, which is analogous to salt-assisted phase separation in saponification processes. In contrast, the –COOH band shows negligible intensity changes (<1%) in both systems, suggesting that free fatty acid neutralization did not play a significant role under the studied conditions. Notably, the aqueous phase in the presence of SS exhibits markedly stronger C–H stretching bands, indicating an increased dispersion of aliphatic

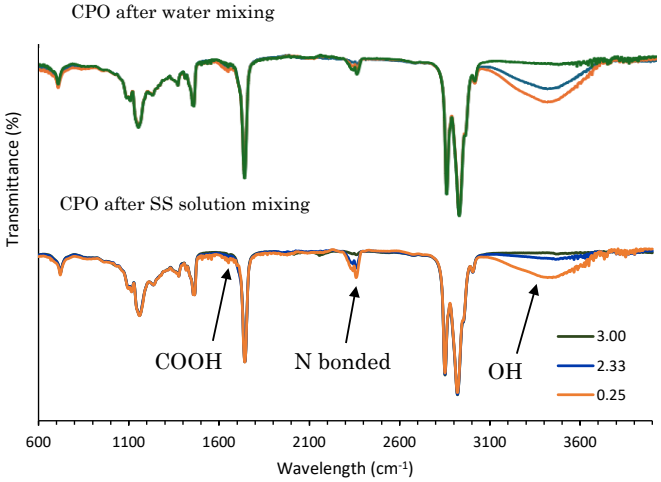

Figure 2. The spectra of crude palm oil for three volume ratios (0.25 for 1:4, 2.33 for 7:33 and 3.00 for 3:1) after being mixed with deionized water and SS solution.

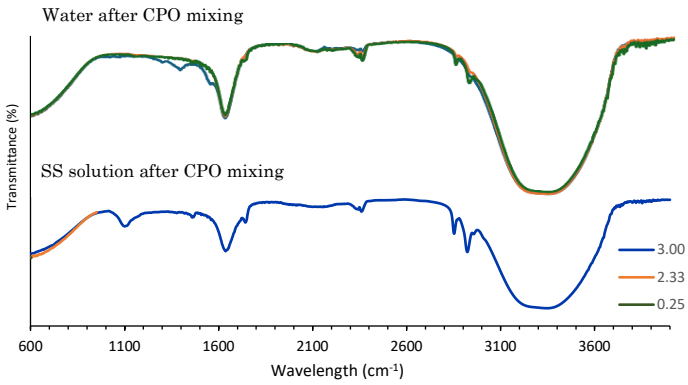

Figure 3. The spectra of water (control) and aqueous phase for three volume ratios (0.25 for 1:4, 2.33 for 7:33 and 3.00 for 3:1) after being mixed with CPO.

compounds within the aqueous medium. This observation is consistent with the formation of a more distinct and stable emulsion, supporting the hypothesis that SS exhibits dispersant or mild surfactant-like behavior [21]. Such enhanced interfacial contact between oil and aqueous phases is expected to improve mass transfer efficiency during dechlorination, thereby contributing to the observed reduction in chlorine content without substantially altering the fatty acid profile of the oil [22].

3.3. Rate of Dechlorination Reaction

The dechlorination of crude palm oil (CPO) proceeded via a nucleophilic substitution mechanism, where the hydroxide ion (OH^-) acted as the primary electron donor. In this study, we characterized the apparent reaction kinetics by tracking the depletion of hydroxide ions, utilizing real-time pH monitoring as a proxy for ion activity. By applying the relationship defined in Equation (4) the measured pH values were converted into corresponding molar concentrations, C_{OH}, allowing for a quantitative assessment of the reaction's progress.

$$C_{OH} = 10^{(pH-14)}, \text{ in mol/L} \quad (4)$$

The reaction was carried out in a batch-stirred, batch reactor model under conditions assumed to be pseudo-homogeneous. The rate of hydroxide consumption ($-r_{OH}$) is defined by the general rate law shown in Equation (5).

$$\frac{dC_{OH}}{dt} = r_{OH} = kC_{OH}^{\propto} \quad (5)$$

Figure 4 illustrates the time-dependent depletion of hydroxide ions during the dechlorination process across three reaction temperatures, i.e. 60 °C, 70 °C, and 80 °C. The decay profiles were fitted using an exponential decay model with a residual intercept as shown in Equation (6).

$$C_{OH} = C_{OH0} + ae^{-bt} \quad (6)$$

The regression analysis demonstrated a high goodness-of-fit ($R^2 > 95$) with standard deviations below 0.1%, confirming that the exponential decay model adequately captures the concentration trends. Unfortunately, the Sigmaplot graphs in Figure 4 cannot show the

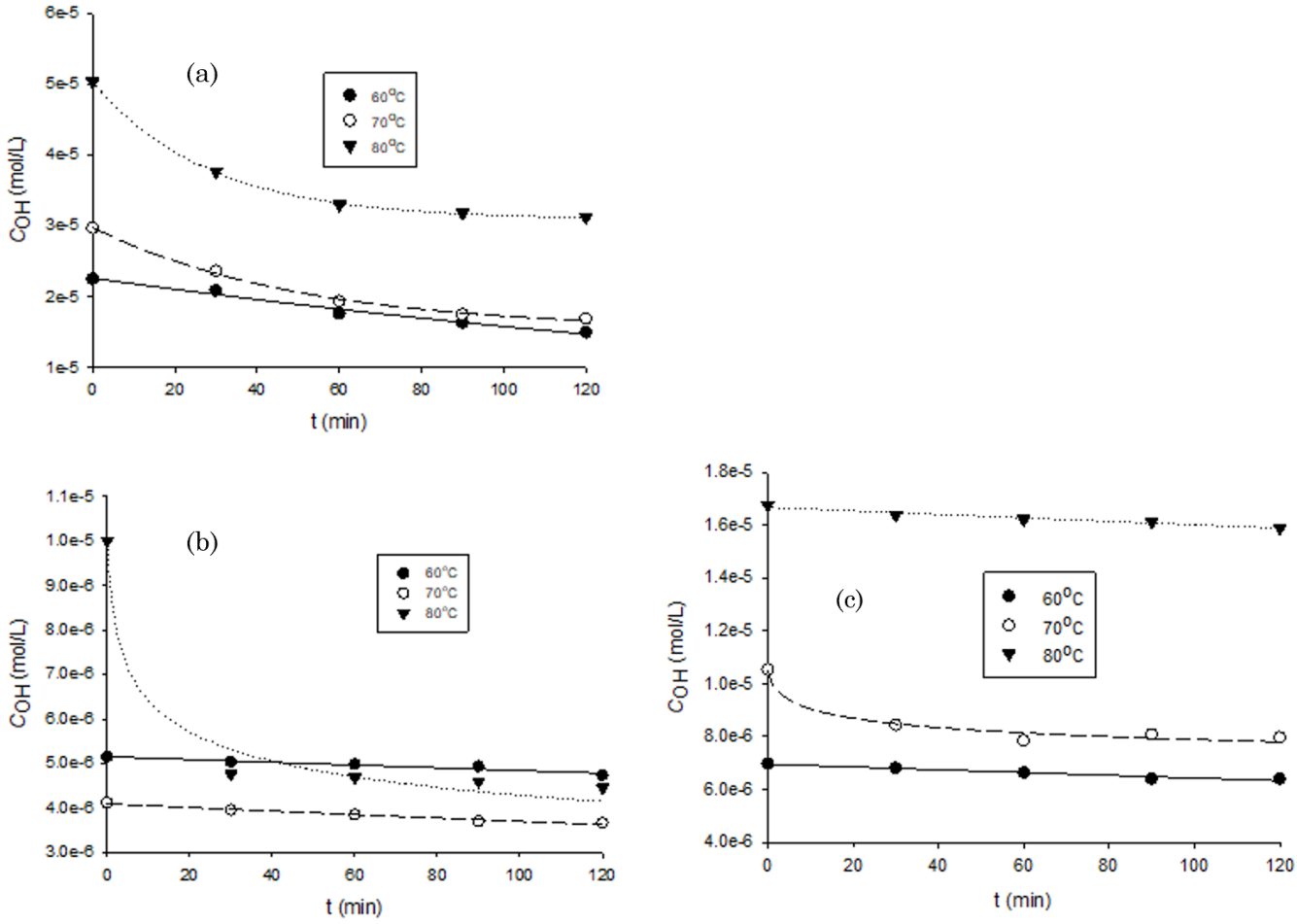

Figure 4. Concentration of hydroxide ion versus reaction time at three reaction temperatures for the CPO: SS solution volume ratio of (a) 1:4, (b) 7:3 and (c) 3:1.

error bars of deviation from various replicates. The utilization of real-time pH monitoring as a proxy for hydroxide ion activity demonstrates the practical application of SS as a buffering agent. As the nucleophilic substitution progresses, the SS solution consistently replenishes OH^- ions through its dissociation equilibrium, thereby maintaining the pH stability required for the continuous conversion of organic chlorides. This buffering mechanism is essential for sustaining the reaction rate under various thermal conditions while preventing the localized acidity that could lead to the formation of corrosive hydrogen chloride.

To determine the kinetic parameters, the rate data were linearized according to the logarithmic form of the power law shown in Equation (7) where the reaction rates were determined by differentiating Equation (6).

$$\log\left(-\frac{dC_{OH}}{dt}\right) = \propto \log C_{OH} + \log k \quad (7)$$

Table 1 also summarizes the kinetic parameters. A pseudo-first-order regime ($\alpha = 1$) was observed for the 1:4 volume ratio at 60 °C, and for the 7:3 and 3:1 ratios at specific temperatures. In these regimes, the rate constants ranged from 4.0×10^{-4} to 3.6×10^{-3} mol.L^{-1}.min^{-1}, suggesting a reaction controlled by conventional nucleophilic substitution. However, significantly higher apparent reaction orders ($\alpha > 3$, reaching up to 24.9) were calculated for the 1:4 ratio at elevated temperatures (70–80 °C) and the 7:3 ratio at 80 °C. Pre-exponential factors and activation energy determinations through the Arrhenius equation are not possible due to inconsistencies of the reaction orders at three different reaction temperatures for each volume ratio. The exceptionally high apparent reaction orders, which exceeded 3 and reached values as high as 24.9 at temperatures between 70 and 80 °C, indicate a profound deviation from elementary kinetic control. While such extreme values in a biphasic liquid-liquid system are often attributed to mass-transfer resistance, the observed precipitous increase in the reaction rate suggests the presence of an autocatalytic mechanism. In this context, the dechlorination process likely generates an intermediate or product that actively facilitates further reaction at the oil-water interface, creating a self-accelerating feedback loop [23]. This behavior is consistent with the sigmoidal kinetic trends previously identified in sodium silicate systems, where the rate of chlorine removal increases as the reaction progresses [11]. The emergence of these high reaction orders effectively reflects this acceleration, as the system moves beyond standard power-law dependencies into a regime governed by product-induced catalysis. Furthermore, the inconsistencies in reaction orders across the three investigated temperatures for each volume ratio make the determination of activation energy and pre-exponential factors through the Arrhenius equation impossible. This suggests that the thermal activation of the reactants is no longer the sole rate-determining factor; instead, the chemical environment at the interface is being modified by the reaction itself [12]. Such autocatalytic behavior may stem from the formation of specific silicate-soap complexes that lower interfacial tension or increase the effective concentration of nucleophiles at the reaction site. This interpretation aligns with established findings regarding 3-MCPD mitigation, which emphasize that the availability and activity of the nucleophile at the oil-water interface dictate the overall kinetics rather than the bulk concentrations of the reactants [24]. Consequently, the high apparent orders serve as a kinetic signature of a system that has transitioned from simple diffusion or thermal control to a more complex, self-promoting chemical pathway.

Table 1. Summary of apparent kinetic parameters based on the power law model.

Volume ratio (CPO: SS)	Temperature (°C)	$C_{OH0} \times 10^6$ (mol/L)	$a \times 10^6$	$b \times 10^3$	Apparent order (α)	Rate Constant (k)
1:4	60	-	22.617	3.6	1.00	3.6×10^{-3}
	70	15.283	14.504	20.0	17.89	2.2×10^{-82}
	80	30.947	19.5	35.9	24.90	1.0×10^{-111}
7:3	60	-	5.153	0.6	1.00	6.0×10^{-4}
	70	-	4.092	1.0	1.00	1.0×10^{-3}
	80	4.57	5.43	111	11.52	3.55×10^{-51}
3:1	60	-	6.963	0.8	1.00	8.0×10^{-4}
	70	7.948	2.593	58.5	3.86	9.72×10^{-10}
	80	-	16.678	0.40	1.00	4.0×10^{-4}

Furthermore, the variation in rate constants across temperatures confirms that the dechlorination efficiency is highly sensitive to the physical state of the mixture. The use of alkaline agents like SS not only provides the necessary nucleophiles but also alters the interfacial tension, thereby influencing the contact area between the chloride precursors and the extracting phase [25].

4. Conclusions

This study provides a comprehensive delineation of the apparent reaction kinetics and extraction performance of SS acting as a chemical scavenger for CPO dechlorination. Our experimental data identifies the 2.33 CPO-to-SS volume ratio as the most effective configuration, achieving a peak chloride extraction of 10,600 ppm. We have demonstrated that SS serves a dual purpose: it functions as a buffering agent that maintains pH stability for the conversion of chlorides into water-soluble forms, while simultaneously acting as a dispersant that reduces interfacial tension to promote better oil-aqueous contact. Furthermore, the data indicates that 80°C is the superior operating temperature for this dechlorination process, as evidenced by the maximized apparent rate constants recorded under these thermal conditions. The study observed a transition in kinetic behavior; while specific conditions followed a pseudo-first-order mechanism (α = 1), elevated temperatures and certain volume ratios resulted in exceptionally high apparent reaction orders up to 24.90, indicating a mass-transfer limited process. Furthermore, a volume ratio of 0.25 (1:4) was found to facilitate the breakdown of chloride ions with the highest rate constant. The results revealed that the kinetic rate is: $r = kC_{OH}^{\propto}$, with the rate constant, k (range 3.6×10^{-3} until 1×10^{-111}) and the apparent order, $\propto$ (range up to 24.9) at 80 ºC. These results confirm that SS provides a water-efficient and effective alternative to conventional washing for mitigating 3-MCPD precursors. For industrial implementation, a higher CPO-to-SS ratio is recommended to optimize extraction while minimizing unwanted soap formation from free fatty acids.

Acknowledgment

The authors gratefully acknowledge the Ministry of Higher Education Malaysia for the financial support provided under the Fundamental Research Grant Scheme (FRGS) with grant number FRGS/1/2022/TK05/UMP/02/23 (RDU220114). Deep appreciation is also extended to LCSB Lepar Hilir Mill and FGVPISB Lepar Hilir Mill for their generosity in supplying the crude palm oil (CPO) samples essential to this research. Finally, the authors thank the Faculty of Chemical and Process Engineering Technology and the Centre of Research in Advanced Fluid and Process (Fluid Centre) at Universiti Malaysia Pahang Al-Sultan Abdullah for providing the facilities and technical support necessary to complete this study.

Declaration

The generative AI and AI-assisted technologies were used in this manuscript to improve the clarity of writing and language.

CRedit Author Statement

Author Contributions: Z.K.U. Hari: Conceptualization, Methodology, Investigation, Resources, Data Curation, Writing, Review and Editing, Supervision; N.S. Rasad: Conceptualization, Methodology, Formal Analysis, Data Curation, Writting Draft Preparation, Visualization; M.S. Mahmud: Validation, Writing, Review and Editing, Data Curation, Investigation. All authors have read and agreed to the published version of the manuscript.

References

[1] Wöhrlin, F., Fry, H., Lahrssen-Wiederholt, M., Preiß-Weigert, A. (2015). Occurrence of fatty acid esters of 3-MCPD, 2-MCPD and glycidol in infant formula. *Food Additives & Contaminants: Part A*, 32(11), 1810-1822. DOI: 10.1080/19440049.2015.1071497

[2] Chew, C.L., Kong, P.S., Chan, E.-S. (2021). Aerobic Liquor Washing Improves the Quality of Crude Palm Oil by Reducing Free Fatty Acids and Chloride Contents. *European Journal of Lipid Science and Technology*, 123(8), 2000347. DOI: 10.1002/ejlt.202000347

[3] Huamán, L., Huincho, S., Aguirre, E., Rodriguez, G., Brandolini, A., Hidalgo, A. (2022). Physico-chemical characteristics and oxidative stability of oils from different Peruvian castor bean ecotypes. *Grasas y Aceites*, 73(1), e445. DOI: 10.3989/gya.1016202

[4] Parveez, G.K.A., Hishamuddin, E., Loh, S.K., Abdullah, M.O., Salleh, K.M., Bidin, M.N.I.Z., . . . Idris, Z. (2020). Oil Palm Economic Performance in Malaysia and R&D Progress in 2019. *Journal of Oil Palm Research*, 32(2), 159-190.

[5] Wu, B., Li, X., Li, Y., Zhu, J., Wang, J. (2016). Hydrolysis Reaction Tendency of Low-Boiling Organic Chlorides To Generate Hydrogen Chloride in Crude Oil Distillation. *Energy & Fuels*, 30(2), 1524-1530. DOI: 10.1021/acs.energyfuels.5b02926

[6] Elisaberh, J. (2023). Mitigation of 3-MCPDE and GE in palm oil in Indonesia. *E-Journal Menara Perkebunan*, 91. DOI: 10.22302/iribb.jur.mp.v91i2.549

[7] Yoon, W., Lee, S., Noh, Y., Park, S., Kim, Y., Ju Kim, H., . . . Bae Kim, W. (2020). Highly Selective Catalytic Dechlorination of Dichloromethane to Chloromethane over Al–Ti Mixed Oxide Catalysts. *ChemCatChem*, 12(20), 5098-5108. DOI: 10.1002/cctc.202000879

[8] Yao, J., Li, Y., Srinivasakannan, C., Ran, J., Li, S., Yin, S., Zhang, L. (2022). Extraction of chloride from slag flush wastewater using solvent N235. *Hydrometallurgy*, 213, 105934. DOI: 10.1016/j.hydromet.2022.105934

[9] Fakher, S., Abdelaal, H., Elgahawy, Y., Imqam, A. (2019). A characterization of different alkali chemical agents for alkaline flooding enhanced oil recovery operations: an experimental investigation. *SN Applied Sciences*, 1(12), 1622. DOI: 10.1007/s42452-019-1662-2

[10] Jaganathan, K., Azman, S.N.F., Umani, Z.K., Abdullah, S.B., Jamari, S.S., Mat, C.R.C., Mahmud, M.S. (2025). Effect of sodium silicate on chlorine content of palm oil. *AIP Conference Proceedings*, 3225(1). DOI: 10.1063/5.0265661

[11] Hari, Z.K.U., Abdullah, S.B., Jamari, S.S., Che Mat, C.R., Mahmud, M S. (2024). Biphasic crude palm oil dechlorination: Effect of volume ratio and concentration of sodium silicate to hydroxide ion distribution. *IIUM Engineering Journal*, 25(1), 47-58. DOI: 10.31436/iiumej.v25i1.2882

[12] Hari, Z.K.U., Abdullah, S.B., Jamari, S.S., Mat, C.R.C., Mahmud, M S. (2025). Effect of sodium silicate solution on total chlorine of crude palm oil under biphasic conditions. *The 3rd Energy Security and Chemical Engineering Congress* (ESChE 2023).

[13] Ramli, M.R., Tarmizi, A.H.A., Hammid, A.N.A., Razak, R.A.A., Kuntom, A., Lin, S.W., Radzian, R. (2020). Preliminary Large Scale Mitigation of 3-Monochloropropane-1, 2-diol (3-MCPD) Esters and Glycidyl Esters in Palm Oil. *J. Oleo. Sci.*, 69(8), 815-824. DOI: 10.5650/jos.ess20021

[14] Ng, M.H., Che Rahmat, C.M., Hasliyanti, A. (2025). Determination of potential chloride contaminants throughout palm oil milling by 35-Cl nuclear magnetic resonance. *Journal of Food Composition and Analysis*, 141. DOI: 10.1016/j.jfca.2025.107368

[15] Fogler, H.S. (2020). Collection and Analysis of Rate Data. In Elements of Chemical Reaction Engineering (5 ed., pp. 256). New Jersey: Prentice-Hall International Inc.

[16] Che Man, Y.B., Aye, W.W., Tan, C.P., Abdulkarim, S.M. (2009). Determination of free fatty acids in crude palm oil, bleached palm oil abd bleached deacidifed palm oil by Fourier Transform Infrared Spectroscopy. *Journal of Food Lipids*, 16(4), 475-483. DOI: :10.1111/j.1745-4522.2009.01160.x

[17] Rozali, N.L., Azizan, K.A., Singh, R., Syed Jaafar, S.N., Othman, A., Weckwerth, W., Ramli, U.S. (2023). Fourier transform infrared (FTIR) spectroscopy approach combined with discriminant analysis and prediction model for crude palm oil authentication of different geographical and temporal origins. *Food Control*, 146, 109509. DOI: 10.1016/j.foodcont.2022.109509

[18] Ng, J.S., Muhammad, S.A., Ibrahim, B., Rafatullah, M., Strashnov, I., Yong, C.H., . . . Ogundipe, O. (2025). Fatty Acid Diagnostic Ratios to Screen for Used Oil Adulteration in Refined, Bleached, Deodorised Palm Oil. *Food Analytical Methods*, 18(8), 1685-1698. DOI: 10.1007/s12161-025-02815-w

[19] Billa, S., Vislavath, P., Bahadur, J., Rath, S.K., Ratna, D., Manoj, N.R., Chakraborty, B.C. (2023). Imparting Reprocessability, Quadruple Shape Memory, Self-Healing, and Vibration Damping Characteristics to a Thermosetting Poly(urethane-urea). *ACS Applied Polymer Materials*, 5(4), 3079-3095. DOI: 10.1021/acsapm.3c00225

[20] Zhu, H., Chen, Y., He, B., Chen, Q., Malik, H., Wang, Y., . . . Liu, Y. (2024). Effects of NaIO4 treatment on the chemical and physical properties of polyacrylonitrile fibers. *International Journal of Polymer Analysis and Characterization*, 29(1), 1-14. DOI: 10.1080/1023666X.2023.2295630

[21] Elmore, A.R. (2005). Final report on the safety assessment of potassium silicate, sodium metasilicate, and sodium silicate. *Int. J. Toxicol.*, 24, Suppl 1, 103-117. DOI: 10.1080/10915810590918643

[22] Singh, J., Soni, H., Kaur, M., Verma, M., Bhattu, M. (2024). Recent advances in the production of soap from used cooking oil for environment remediation. *E3S Web of Conferences*, 509. DOI: 10.1051/e3sconf/202450903014

[23] Yuen, C.S., Fui, K.H., Wren, W.G. (2006). Autocatalytic hydrolysis and autooxidation of crude palm oil under various constant humidities. *Journal of Oil Palm Research*, 18, 278-287.

[24] Ganasen, P., Khan, M.R., Kalam, M.A., Mahmud, M.S. (2014). Effect of visible light on catalytic hydrolysis of p-nitrophenyl palmitate by the Pseudomonas cepacia lipase immobilized on sol-gel support. *Bioprocess Biosyst. Eng.*, 37(11), 2353-2359. DOI: 10.1007/s00449-014-1213-6

[25] Amiri, H.A.A. (2017). Improvement of Water Displacement Efficiency in Sandstone Reservoirs Using Buffered Sodium Silicate. *Journal of Porous Media*, 20(3), 193-203. DOI: 10.1615/JPorMedia.v20.i3.10